

This article was downloaded by: [University Of Pittsburgh], [Jiho Song]

On: 23 November 2013, At: 11:20

Publisher: Taylor & Francis

Informa Ltd Registered in England and Wales Registered Number: 1072954 Registered office: Mortimer House, 37-41 Mortimer Street, London W1T 3JH, UK



Journal of Adhesion Science and Technology

Publication details, including instructions for authors and subscription information:

<http://www.tandfonline.com/loi/tast20>

Enhanced fabrication and characterization of gecko-inspired mushroom-tipped microfiber adhesives

Jiho Song^a, Yigit Mengüç^a & Metin Sitti^a

^a Department of Mechanical Engineering, Carnegie Mellon University, Pittsburgh, PA, 15213-3890, USA

Published online: 25 Feb 2013.

To cite this article: Jiho Song, Yigit Mengüç & Metin Sitti (2013) Enhanced fabrication and characterization of gecko-inspired mushroom-tipped microfiber adhesives, Journal of Adhesion Science and Technology, 27:17, 1921-1932, DOI: [10.1080/01694243.2013.766533](https://doi.org/10.1080/01694243.2013.766533)

To link to this article: <http://dx.doi.org/10.1080/01694243.2013.766533>

PLEASE SCROLL DOWN FOR ARTICLE

Taylor & Francis makes every effort to ensure the accuracy of all the information (the "Content") contained in the publications on our platform. However, Taylor & Francis, our agents, and our licensors make no representations or warranties whatsoever as to the accuracy, completeness, or suitability for any purpose of the Content. Any opinions and views expressed in this publication are the opinions and views of the authors, and are not the views of or endorsed by Taylor & Francis. The accuracy of the Content should not be relied upon and should be independently verified with primary sources of information. Taylor and Francis shall not be liable for any losses, actions, claims, proceedings, demands, costs, expenses, damages, and other liabilities whatsoever or howsoever caused arising directly or indirectly in connection with, in relation to or arising out of the use of the Content.

This article may be used for research, teaching, and private study purposes. Any substantial or systematic reproduction, redistribution, reselling, loan, sub-licensing, systematic supply, or distribution in any form to anyone is expressly forbidden. Terms & Conditions of access and use can be found at <http://www.tandfonline.com/page/terms-and-conditions>

Enhanced fabrication and characterization of gecko-inspired mushroom-tipped microfiber adhesives

Jiho Song, Yigit Mengüç and Metin Sitti*

Department of Mechanical Engineering, Carnegie Mellon University, Pittsburgh, PA 15213-3890, USA

(Received 7 January 2012; final version received 7 December 2012; accepted 7 January 2013)

Geckos exhibit a unique ability to adhere repeatedly and reversibly to a variety of surfaces. Considerable scientific and engineering efforts over the last decade have produced gecko-inspired adhesives which can outperform the gecko in some regards. However, the best results come from adhesives which are difficult to mass-produce, or degrade through repeated use. Here, we propose a method for fabricating micrometer-scale, gecko-inspired adhesive structures with mushroom tips in densely packed arrays using deep reactive ion etching (DRIE) and soft mold replication. We use xenon difluoride etching to release the cured polymer structures from the DRIE-processed silicon wafer, and soft mold replication to avoid surface fluorination in the final adhesive patches. The patterned adhesives exhibit more than an order of magnitude increase in pull-off force compared to an unstructured, flat control sample. More importantly, the adhesives' structures retain 80% of their original attachment strength through repeated use, even after 1000 contact cycles. To investigate the importance of three parameters described in theoretical works, we characterize the effect of boundary conditions on friction, the effect of backing layer on pull-off force, and the effect of retraction speed on pull-off force. Our fabrication approach could be used to mass produce wafer-size patches of structured adhesive that exhibit higher repeatability and the utilized experimental adhesive characterization methods will allow better optimization of future gecko-inspired adhesive designs.

Keywords: gecko-inspired; dry adhesion; repeatability; surface fluorination

1. Introduction

In the last decade, scientists have found the true mechanisms of gecko foot-hairs adhesion [1,2] and engineers have attempted to fabricate synthetic fibrillar adhesives, achieving even higher adhesion strengths than the real gecko footpads.[3–6] However, high adhesive strength is the only one criterion in matching the performance of gecko foot-hairs; we must also consider repeatability, directionality, reliability, and efficiency.[7] Adhesive surfaces that provide strong, repeatable attachment have possible applications in medical devices,[8,9] the feet of climbing robots,[10,11] as robotic manipulators,[3] and as an alternative to hook-and-loop or mechanical fasteners in clothing. The key for these applications is to have an adhesive that provides the same strong attachment through hundreds or thousands of repeated uses and is mass producible.[2,12,13]

Researchers of synthetic gecko adhesives have used a variety of fabrication techniques and materials in an attempt to mimic more closely the structure of gecko foot hairs, but the most common approach is through soft lithography, a process formalized by Whitesides

*Corresponding author. Email: msitti@andrew.cmu.edu

et al. [14] and first exploited by Sitti and Fearing [15] to fabricate synthetic fibrillar adhesives through silicone rubber micromolding. Geim et al. [16] demonstrated the fabrication of polyamide nanofiber arrays produced by electron-beam lithography. After these initial fabrication works, simple vertical fiber arrays were fabricated from various materials such as polymers and carbon nanotubes.[17,18] SU-8 based lithography can produce sharp clean side walls and high aspect ratio fibers, but is generally limited to fibers tens of microns in diameter.[19] Techniques such as deep reactive ion etching (DRIE), also called the Bosch process, allow for smaller structure on the order of hundreds of nanometers in diameter and even lead to mushroom-shaped tip endings due to the notching effect. Kim et al. [20] and Jeong et al. [3] have demonstrated techniques for forming flat mushroom tips of more complex 3D geometries using DRIE. Kim et al. [20] showed it was possible to exploit the notching effect [21] observed when silicon is isotropically etched at the interface with an etch-resistant layer of material (e.g. silicon dioxide) to create spatular tips on microfibers.[22] Jeong et al. [23,24] demonstrated the fabrication of angled nanopillars with spatular tips through DRIE and the addition of a Faraday cage to help angle the ion paths incident to the etched silicon. For both groups' approaches, the unsolved problem lies not in fabricating the negative templates through DRIE, but in molding and releasing large patches of micro or nanopillars which can robustly act as an adhesive surface. The results of micro-structured adhesives' fabrication have been fruitful in producing novel synthetic facsimiles but there has been a lack of focus on taking these structures to a mature, industrial application level.

Among all the approaches taken to create synthetic gecko adhesives, we chose to use DRIE in producing fiber arrays because the notching effect can be utilized to form mushroom-shaped tips on released polymer fibers. This approach to fabricating polymer fiber arrays has the following advantages with respect to other fibrillar adhesive fabrication methods: (1) cost effectiveness thanks to fabrication in large areas (up to 12 inch wafer size) using a single mask; (2) high yields reaching nearly 100%; and (3) the fiber material can be selected independently because of the process of casting polymer to the negative mold template. The structures have a $5.28\ \mu\text{m}$ stem diameter, a mushroom-shaped tip that is $9.62\ \mu\text{m}$ in diameter, and a height of $20\ \mu\text{m}$. Previously, we used DRIE to produce a similar adhesive structure, but releasing the molded elastomer structure had required a Xenon Difluoride (XeF_2) etch which had resulted in surface fluorination of the elastomer which reduced the repeatability of adhesion.[20] Surface-fluorinated polymer surface can have desirable properties in certain cases, including: (1) decreased gas permeability (increased barrier properties); (2) decreased friction (decreased wear and elongated lifetime); and (3) enhanced hardness.[25,26] Although surface fluorination caused fiber tips to be more adhesive initially, the fluorinated layer on the tips would peel off the fibers and remain on contact surfaces as residue. To address the issue of surface fluorination, we present a multiple-molding process to fabricate the negative silicone rubber mold. Creating a negative mold gives us flexibility to choose the adhesive material from a wide range of polymers, and permits the same mold to be used hundreds of times, increasing fabrication speeds and reducing cost.

We show that our method results in repeatable adhesion with consistent adhesion strength over a thousand cycles of attachment–detachment. The adhesive behavior of the structure was characterized on a custom system, and includes investigating the adhesion as related to repeated trials, unloading rates, and backing layer thickness. The friction behavior is also investigated under constant compressive load and constant compressive displacement conditions to address recent theoretical work that showed that microstructure stability changes as boundary conditions change.[27]

2. Fabrication

2.1. Wafer scale fabrication of single-level polymer microfiber arrays with mushroom-shaped tips

The notching effect in the DRIE fabrication process (STS Multiplex ICP RIE) allows control over the spatula tip diameter by varying the lateral etching time. This technique enabled fabrication of microfiber arrays of sizes up to a four-inch wafer inexpensively with high yields and was advantageous in comparison to other proposed fibrillar adhesive fabrication techniques. We used silicon-on-insulator (SOI) wafers as a substrate for microfiber arrays. Each SOI wafer had a 20 μm thick top silicon (Si) layer, a 1 μm thick silicon dioxide (SiO_2) layer, and a 600 μm thick Si-handling layer. An individual 15 \times 15 mm^2 SOI chip was used to create the negative mold for fabrication of the first microfiber array. In this modified method, we mold the first microfiber array to silicone rubber to create a second negative mold which was used to finally cast microfiber arrays without surface fluorination.

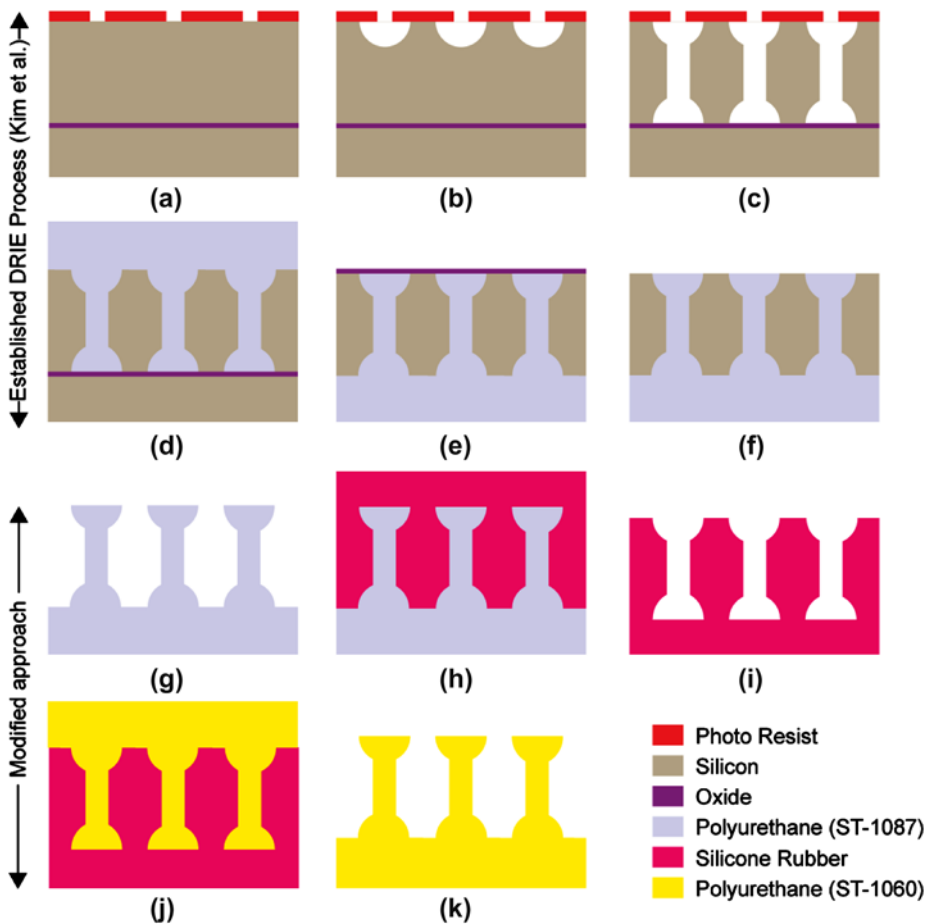


Figure 1. Schematic fabrication flow steps: ((a)–(c)) DRIE produces a negative mold template in an SOI wafer; ((d)–(g)) Molding of the first positive polymer microfiber array; ((h)–(k)) Additional steps to create a negative mold template in silicone rubber helped to avoid surface fluorination of the final positive polymer microfiber array.

The initial fabrication process was carried out by following Kim et al.'s [20] procedure for fabricating the negative Si mold with mushroom-shaped tips (Figure 1(a)–(c)). The additional steps avoided surface fluorination on the tip of the final microfiber,[26] in which the surface properties of the released top surface (Figure 1(f)) would change due to exposure to XeF_2 .

In Figure 1(c)–(d), an etched Si single-layer microscale fiber array was filled with a liquid polyurethane elastomer (ST-1087; BJB Enterprises, Tustin, CA) under vacuum, and then the polymer was cured 24 h in ambient temperature and humidity. In Figure 1(e)–(f), the cured polymer microfiber array with a backing layer was released via a three-step etching process as introduced by Kim et al. [20]. In Figure 1(h), the released polymer microfiber array was covered with liquid silicone rubber (HS-II, Dow Corning, Midland, MI), and allowed to cure at ambient temperature for seven days. Once cured, the silicone rubber was carefully peeled from the polymer microfiber array, resulting in a flexible silicone rubber mold with the negative image of the microfiber array shape (Figure 1(i)). Then, in Figure 1(i)–(j), liquid polymer (ST-1087) was poured into the negative silicone rubber mold and placed under vacuum to remove the trapped air bubbles, before being cured at ambient temperature for 2–7 days. After demolding, the positive polyurethane microfibers had exactly the same geometry as the original microfibers, Figure 1(k). Imaging the resulting microfibers with a scanning electron microscope (SEM) (2460 N, Hitachi) revealed microfiber arrays with 5.28 μm fiber-stem diameter, 9.62 μm tip diameter, 10 μm base diameter, 20 μm length, and 12 μm center-to-center spacing between each fiber in a square packing arrangement (78% fiber tip area density), as shown in Figure 2. To avoid fiber collapse, the rubber mold and cast polymer were cooled to below 4 $^\circ\text{C}$ temperature for one hour before the cast polymer was gently peeled from the silicone rubber mold. However, successful demolding of high aspect ratio polyurethane microfiber arrays without breaking the fibers was a significant challenge and required great care.

In order to characterize normal adhesion and friction properties, fiber arrays were molded on flat glass substrates which acted as handling layers. An acrylic window with the thickness of 550 μm was used as a spacer between the negative silicone rubber mold and the glass handling layer during the molding process to control the thickness of the polymer backing layer. It was important to control the backing layer thickness because of the effect it can have on adhesion.[28]

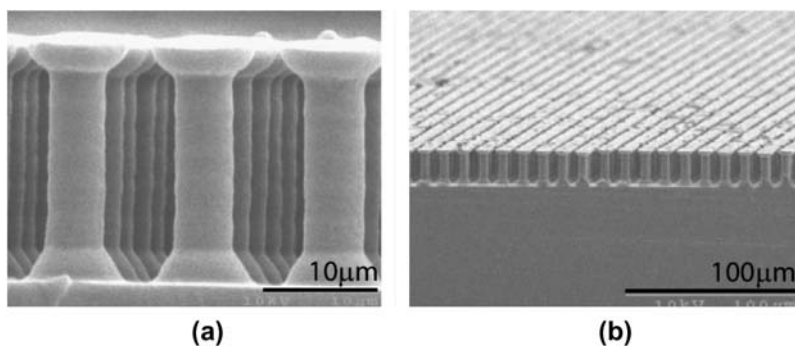


Figure 2. SEM images of polyurethane elastomer microfiber arrays; (a) (scale bar: 10 μm). (b) (Scale bar: 100 μm).

3. Experimental methodology

3.1. Experimental setup

The performance of microscale fiber arrays was characterized by measuring macroscale pull-off forces. The adhesive forces for a $15 \times 15 \text{ mm}^2$ area with $550 \mu\text{m}$ thick backing-layer structured samples and a $550 \mu\text{m}$ thick flat smooth unstructured surface were measured for several preloads. The flat polyurethane surface was used as a control substrate to show the relative adhesion enhancement by structuring the same material with mushroom-tipped microfibers. Experimental adhesion data from the microfiber arrays were compared with Kim et al.'s [20] microfiber arrays.

The custom macroscale adhesion (pull-off) measurement system was based upon the load-drag-pull adhesion and friction characterization system similar to several prior works. [18,29–32] It consisted of an inverted view optical microscope (Nikon Eclipse TE200, Melville, NY) with an automated stage (MFA-CC; Newport, Irvine, CA), which held a load cell (GSO-25; Transducer Technique Inc., Tamecula, CA). A 6 mm diameter (QU-HS-12; ISP Optics, Irvington, NY) glass hemisphere was attached to an acrylic cantilever-beam mounted to the load cell and used as an indenter. A hemisphere shape was used in order to eliminate alignment errors during experiments. Custom real-time software controlled the stage's motion, bringing the hemisphere into contact with the fiber sample at a fixed velocity of $1 \mu\text{m/s}$ until a specified compressive force, called the preload, was reached. After 1 s contact time, the hemisphere was retracted at $1 \mu\text{m/s}$ until it fully separates from the sample. During retraction, the magnitude of the maximum tensile force corresponded to the adhesion.

For the friction tests, the 6 mm diameter smooth glass hemisphere was brought into contact at $1 \mu\text{m/s}$ with the fiber sample which was mounted directly onto a second load cell configured for lateral sensing and motion. Once the preload was reached, the fiber sample was dragged laterally along the hemisphere at a $1 \mu\text{m/s}$ for 300 s. The maximum lateral force was defined as the friction force. The friction forces were measured in two different preload regimes, constant compressive displacement, and constant compressive load.

4. Characterization results and discussion

Here, we present five experiments to characterize our microfiber arrays. These measurements show that our adhesives are robust, repeatable, and potentially energy-efficient temporary attachment mechanisms that could be used in many different types of devices.

4.1. Adhesion enhancement

The adherence of an array of fibers is not simply the product of the number of fibers in the array and the single fiber adherence. Fiber array adhesion is a function of many parameters such as fiber geometry, fiber spacing, and surface topography of the adhering surface.[33] As seen in Figure 3(a), as preload was increased, the adhesion increased and eventually saturated at a steady value due to geometrical and material effects. Geometrically, the hemisphere's real contact area was related to the depth to which it indented the adhesive's surface, and this real contact area approached the limit defined by the surface area of the hemisphere as the indentation depth approached the radius of the hemisphere. Additionally, the increased contact area distributes the preload over more of the adhesive surface which in turn reduces the incremental increase of indentation depth for an incremental increase in preload. An approximate analytical model for short and long vertical fiber array adhesion was well defined to predict the trends and relative performance for fiber arrays.[33] One should note that the saturation of

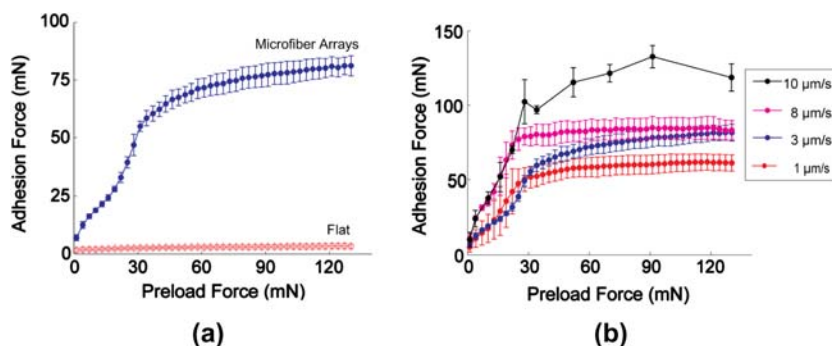


Figure 3. (a) Results of pull-off adhesion of polyurethane elastomer (ST-1087, BJB Enterprise) microfiber arrays at $8\ \mu\text{m/s}$ retraction speed for varying preloads. Each error bar on the graph represents the mean and the standard deviation of measured adhesion on five different areas of the microfiber arrays at the given preload. For adhesion characterization, we maintained the same thickness ($550\ \mu\text{m}$) and pull-off speed to compare the adhesion. (b) Adhesion strength experiment results as a function of retraction speed. Each error bar represents the mean and standard deviation of measured adhesion for three different areas of the fiber arrays at given preloads.

fiber arrays adhesion was not only caused by the geometry, but it may also be caused by the backing layer thickness on single-level microfiber structures.[28,34] These effects together resulted in a saturation of the contact surface area of the hemisphere-adhesive interface and hence a saturation of the adhesion force. Moreover, from Figure 3(a), the adhesion of the flat control sample was higher than that of all the fiber samples. This was likely due to the bulk and surface viscoelastic response of the material. Since Johnson-Kendall-Roberts theory predicted that the adhesion of the flat sample should not change with preload, it is clear from Figure 3(a) that there are significant bulk and surface viscoelastic effects [35] which increase the adhesion of the flat control sample, particularly for high preloads. The compliant microfiber array samples had three to nine times higher adhesion than the stiff, unstructured flat surface. The microfiber array samples were observed to stretch up to 260% of their initial length before detachment, while the backing layer thickness remained undeformed, as shown in Figure 4(a)–(b). Since higher preloading generated a larger contact area and a larger difference in indentation depth between the edge and the center regions of the contact area, the experiments under higher preloads provided insight into the adhesion performance against a rough surface.[36]

4.2. Effect of retraction speed on adhesion

To investigate the effect of viscoelasticity on adhesion, a series of tests that varied the retraction speeds were conducted on arrays of ST-1087 microfibers. The results in Figure 3(b) showed that increased retraction speeds can lead to increased adhesion strength but at the same time, more fiber collapse was observed at $10\ \mu\text{m/s}$, resulting in reduced repeatability of adhesion performance. The saturated adhesion was observed to increase with increased retraction speeds, portraying typical behavior of viscoelastic materials.[35,37] At the highest retraction speed, adhesion increased by up to 220% for equivalent preloads (Figure 3(b)).

4.3. Effect of backing layer thickness on adhesion

According to the theoretical model in previous studies, a thin backing layer promotes adhesion by allowing each individual fiber in contact to bear the same amount of load and satisfy

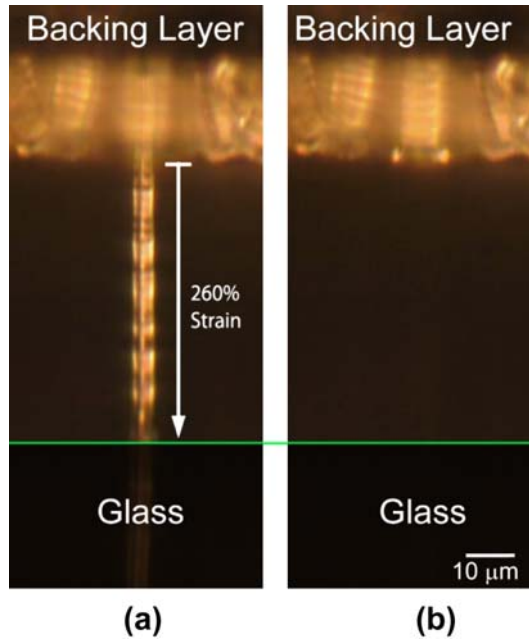


Figure 4. Two video snapshots of microfibers contacting a 6 mm diameter glass hemisphere: (a) During pulling and (b) After detachment.

what is called the Equal Load Sharing (ELS) condition.[28,34] This was proposed by Hui [34] explaining that the difference in which very thin backing layers promote ELS, maximizing adhesion. A more compliant polymer, with a Young's modulus of 2.9 MPa (ST-1060, BJB), was used to characterize the effect of the backing layer thickness. The adhesion measurement system was modified to characterize the pull-off force of microfiber array samples with different backing layer thicknesses. The setup was similar to the aforementioned experimental system but in this case, a 1 mm flat Si circular disk was used as a flat-punch indenter in addition to a 6 mm glass hemisphere. Direct comparison of the different backing layer thickness adhesion between the glass hemisphere and flat Si disk was performed only up to a maximum preload of 20 mN in order to prevent lateral collapse of the fibers.

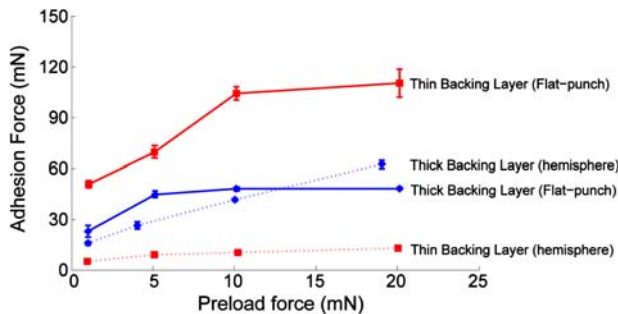


Figure 5. The effect of backing layer thickness on the adhesion of polyurethane (ST-1060, BJB Enterprise) microfiber arrays on a glass hemisphere with 6mm diameter and a silicon disk with 0.50 mm radius (error bars represent five data points for each backing thickness tested at different fiber array locations. The thin backing layer was 22 μm and the thick backing layer was 385 μm).

The results observed in Figure 5 confirmed previous observations regarding the effect of the backing layer on the adhesion force in the case of flat-punch experiments. In the case of a flat Si disk experiment, a thinner backing layer promoted equal sharing of the load by the fibers and each fiber experiences the same vertical tension.[28,34,38,39] When the backing layer was thicker, the deformation of the fiber-backing layer system was dominated by the backing layer, resulting in stress concentration at the edge of the contact and reduced adhesive force.

However, the results in Figure 5 show the opposite relation between backing layer and adhesion when the indenter was a hemisphere instead of a flat-punch. Resultant adhesion of the polyurethane microfiber arrays on a 385 μm thick backing layer was up to three times greater than fiber arrays on a 22 μm thick backing layer when indented with a hemisphere. The hemisphere-indentation experiments revealed the positive relationship between thicker backing layer and increased adhesion, because the thicker backing layer was more compliant and results in more contact between the indenter and adhesive fiber array. This was in contrast to the case of the flat-punch indenter where the increased compliance of the backing layer did not result in increased contact, but instead lead to unequal load sharing between the fibers at the edge of contact and those in the center.

4.4. Repeatability of adhesion

The tests of repeatability were conducted to investigate how the adhesive performance degraded. According to the adhesion vs. preload experiments, microfiber arrays molded with a high elastic modulus material (ST-1087) exhibited more stability at preloads over 100 mN and so this stiffer polymer was used in lifetime testing. Repeatability adhesion tests were performed by loading the same area of the sample over 1000 cycles, with four different preloads, and approach and retraction speeds of 1 $\mu\text{m}/\text{s}$. Figure 6(a) illustrates the change in adhesion over many cycles, with the first cycle exhibiting the highest adhesion and subsequent runs lowering that values lightly. The overall trend of the data in Figure 6(a) suggests that a good adhesion level was maintained more consistently at low preloads and a relatively low speed of retraction as shown in Figure 3(b), while higher preloading caused more significant adhesion degradation, due to fiber collapse. Also, a thick backing layer was used to prevent lateral fiber collapsing. After running multiple adhesion tests in the same area of the fiber array to measure adhesion, the region where indentation occurred turned dark, as illustrated in Figure 6(b)–(c).

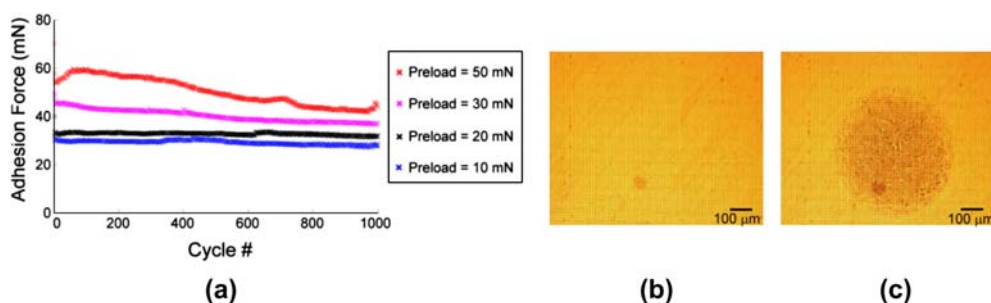


Figure 6. (a) Results of repeatability of adhesion testing for 1000 cycles with mushroom-tip microfibers for 10 mN increments of preloads. Optical microscope's top view images of (b) before and (c) after repeatability adhesion testing for 1000 cycles at a preload of 50 mN.

Kim et al's studies suggested a rapid decline in performance over time as a result of fluorinated polymer surface.[20,26,40] Moreover, in previous work, surface fluorination caused fiber tips to be initially more adhesive and increased the surface energy of the fibers.[20] However, it was observed that adhesion degraded dramatically over consecutive tests and eventually saturated at 20% of the initial adhesion measured value.

Our manufacturing process eliminated fluorination effects and experiments performed on the same microfibers sample of $15 \times 15 \text{ mm}^2$ area over the course of three weeks showed no significant degradation in adhesion. Eliminating fluorination effects resulted in adhesives maintaining over 80% of their original adhesion through a thousand cycles. Figure 6(a) illustrates the consistency of adhesion for preloads of 10 and 20 mN. Higher preloads showed more degradation in adhesion in the earlier cycles, which indicated there was a limit to the physical properties of the material. Possible reasons for adhesion degradation in our results include: lateral fiber collapse (contacting and adhering to neighboring fibers or onto the backing layer), contamination, and changing of the material properties of the polymer over time or due to stress. Once the fiber tips were not oriented toward the contacting surface, fibers were unlikely to provide much adhesion due to the reduced contact area. Microfibers were also observed to change color over multiple loading cycles, as shown in Figure 6(b)–(c). Since the polyurethane used to fabricate the fiber samples has viscoelastic properties, it is likely that these properties, as well as stiffness, change after repeated cycling. We could also observe that after initial detachment occurred, the fibers appeared to soften significantly over the first few cycles and continued to soften for the additional cycles.

4.5. Effects of loading conditions on friction of polymer microfiber arrays

Macroscale frictional characterization of the fabricated ST-1087 fiber arrays was performed using two different boundary conditions during shearing: constant compressive and constant

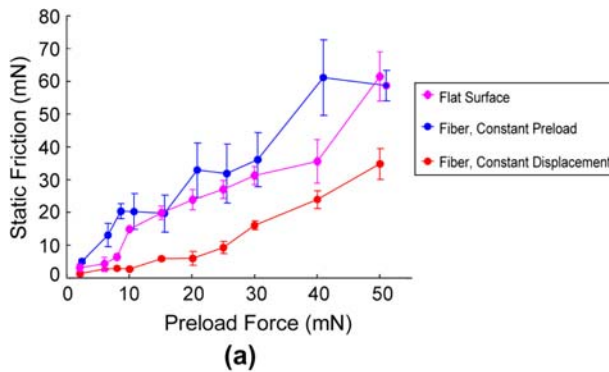


Figure 7. (a) Resulting friction forces for experiments where constant compressive displacement or force is applied to fiber arrays or flat surfaces by a sliding glass hemisphere. Error bars represent the standard deviation for the five trials at each data point. (b) The sidewall contacts of the fibers seen under optical microscope.

compressive displacement. We ensured constant preload force by implementing a proportional-integral-derivative-controller on the z -axis actuator using feedback from the load cell. Figure 7(a)–(b) shows the adhesive friction performance of a polyurethane flat surface and a mushroom-shaped fiber array with the same backing [13] layer thickness (550 μm). The static friction was defined as the peak lateral force before slipping occurred. The static friction of the microfiber arrays appeared to increase linearly with the increasing preload force applied by glass hemisphere. The flat adhesive surface exhibited no significant difference in friction between constant preloading and constant displacement boundary conditions during shearing. However, the mushroom-shaped tip array sample with both constant preloading and constant compressive displacement demonstrated adhesive friction. In contrast, the adhesive friction of constant displacement was measured with the load conditions being displacement driven, meaning that the indentation depth is kept constant during the lateral movement. This setting is kept at all preloads for all fiber samples.

The preload values in Figure 7(a) corresponded to the applied compressive load prior to lateral motion. At every preload, the maximum static friction of the fiber array under constant preload was higher than the maximum static friction of the flat surface. The maximum static friction was considerably higher for the constant compressive preload case than for the constant compressive displacement case. This difference in static friction can be attributed to the behavior of the compliant fibers under the different boundary conditions. When a constant compressive displacement was set, the glass hemisphere moved laterally, the fibers were bent, detached, and finally only made contact with the glass hemisphere along the edges of their top surfaces. However, when a constant compressive preload was set, the fibers were bent and detached but the hemisphere was pressed into the array to maintain the compressive load which resulted in greater contact between the indenter and the sides of the fibers and hence greater friction force was produced.

5. Conclusion

In this study, we presented a method of fabricating large arrays of gecko-inspired microfibers with mushroom-shaped tip endings through the DRIE process coupled with soft polymer molding. We improved a previously presented process and demonstrated that our microfiber arrays had a greatly improved repeatability of adhesion, retaining 80% of their attachment strength after 1000 loading cycles. The appearance of darkening in the adhesive sample seemed to indicate that we are approaching the performance limits of the material, but not the limits of adhesion. We also investigated several parameters that can influence the adhesion and friction performance of synthetic gecko-inspired adhesives. Specifically, we found that a thicker backing layer improved adhesion to a hemisphere punch. In contrast, a thicker backing layer reduced adhesion to a flat cylindrical punch. Additionally, we confirmed that faster pull-off increased the measured adhesive force, but at the cost of damaging the microfiber array which is another limitation imposed by the material strength. Finally, we tested a recent numerical model predicting the behavior of fibers when sheared under different boundary conditions: we found that with constant preload, the fibers exerted a stronger static friction force than when the boundary condition was one of constant displacement. What is important to take away from our findings is that we demonstrated a method to create arrays of micro-scale gecko-inspired fiber adhesives in a way that can be scaled up and replicated. The DRIE is an established microfabrication process, and the soft molding steps we demonstrated are easy to access commercially available mold making rubbers and polyurethanes. There were already limited demonstrations of gecko-inspired adhesives used in medical applications and

robotics, but our focus on making a mass producible gecko tape has the potential to translate the research of this field to real-world commercial products in the future.

Acknowledgments

The authors thank S. Arabagi, B. Aksak, and E. Diller and all other NanoRobotics Laboratory members for fruitful discussions. Thanks are extended to J. Suhan for work on the Scanning Electron Microscope imaging. This work was partially funded by National Science Foundation (CMMI-0800408). Y. Mengüç was partially supported by the Claire and John Bertucci Fellowship.

References

- [1] Autumn K, Liang Y, Hsieh S, Zesch W, Chan W, Kenny T, Fearing R. Adhesive force of a single gecko foot-hair. *Nature*. 2000;405:681–685.
- [2] Autumn K, Sitti M, Liang Y, Peattie A, Hansen W, Sponberg S, Kenny T, Fearing R, Israelachvili J. Evidence for van der Waals adhesion in gecko setae. *Proc. Nat. Acad. Sci. U.S.A.* 2002;99:12252.
- [3] Jeong HE, Suh KY. Nanohairs and nanotubes: efficient structural elements for gecko-inspired artificial dry adhesives. *Nano Today*. 2009;4:335–346.
- [4] Northen MT, Greiner C, Arzt E, Turner KL. A gecko-inspired reversible adhesive. *Adv. Mater.* 2008;20:3905–3909.
- [5] Del Campo A, Greiner C, Álvarez I, Arzt E. Patterned surfaces with pillars with controlled 3D tip geometry mimicking bioattachment devices. *Adv. Mater.* 2007;19:1973–1977.
- [6] Murphy MP, Aksak B, Sitti M. Adhesion and anisotropic friction enhancements of angled heterogeneous micro-fiber arrays with spherical and spatula tips. *J. Adhes. Sci. Technol.* 2007;21:1281–1296.
- [7] Autumn K. How gecko toes stick: the powerful, fantastic adhesive used by geckos is made of nanoscale hairs that engage tiny forces, inspiring envy among human imitators. *American Scientist*. 2006;94:124–132.
- [8] Glass P, Sitti M, Appasamy R. A new biomimetic adhesive for therapeutic capsule endoscope applications in the gastrointestinal tract. *Gastrointest. Endosc.* 2007;65:AB91.
- [9] Glass P, Cheung E, Sitti M. A legged anchoring mechanism for capsule endoscopes using micro-patterned adhesives. *IEEE Trans. Biomed. Eng.* 2008;55:2759–2767.
- [10] Murphy MP, Sitti M. Waalbot: an agile small-scale wall-climbing robot utilizing dry elastomer adhesives. *IEEE/ASME Trans. Mechatron.* 2007;12:330–338.
- [11] Kim S, Spenko M, Trujillo S, Heyneman B, Santos D, Cutkosky MR. Smooth vertical surface climbing with directional adhesion. *IEEE Trans. Rob.* 2008;24:65–74.
- [12] Huber G, Mants H, Spolenak R, Mecke K, Jacobs K, Gorb SN, Arzt E. Evidence for capillarity contributions to gecko adhesion from single spatula nanomechanical measurements. *Proc. Nat. Acad. Sci. U.S.A.* 2005;102:16293.
- [13] Sun W, Neuzil P, Kustandi TS, Oh S, Samper VD. The nature of the gecko lizard adhesive force. *Biophys. J.* 2005;89:L14–L17.
- [14] Xia Y, Whitesides GM. Soft lithography. *Annu. Rev. Mater. Sci.* 1998;28:153–184.
- [15] Sitti M, Fearing RS. Synthetic gecko foot-hair micro/nano-structures as dry adhesives. *J. Adhes. Sci. Technol.* 2003;17:1055–1074.
- [16] Geim A, Grigorieva SVDIV, Novoselov K, Zhukov A, Shapoval SY. Microfabricated adhesive mimicking gecko foot-hair. *Nat. Mater.* 2003;2:461–463.
- [17] Zhao Y, Tong T, Delzeit L, Kashani A, Meyyappan M, Majumdar A. Interfacial energy and strength of multiwalled-carbon-nanotube-based dry adhesive. *J. Vac. Sci. Technol., B: Microelectron. Nanomet. Struct.* 2006;24:331–335.
- [18] Aksak B, Sitti M, Cassell A, Li J, Meyyappan M, Callen P. Friction of partially embedded vertically aligned carbon nanofibers inside elastomers. *Appl. Phys. Lett.* 2007;91:061906.
- [19] Bogdanov A, Peredkov S. Use of SU-8 photoresist for very high aspect ratio x-ray lithography. *Microelectron. Eng.* 2000;53:493–496.
- [20] Kim S, Sitti M. Biologically inspired polymer microfibers with spatulate tips as repeatable fibrillar adhesives. *Appl. Phys. Lett.* 2006;89:261911.
- [21] Li J, Zhang Q, Liu A, Goh W, Ahn J. Technique for preventing stiction and notching effect on silicon-on-insulator microstructure. *J. Vac. Sci. Technol., B: Microelectron. Nanomet. Struct.* 2003;21:2530.

- [22] Northen M, Turner K. A batch fabricated biomimetic dry adhesive. *Nanotechnology*. 2005;16:1159.
- [23] Jeong HE, Lee JK, Kim HN, Moon SH, Suh KY. A nontransferring dry adhesive with hierarchical polymer nanohairs. *Proc. Nat. Acad. Sci.* 2009;106:5639–5644.
- [24] Jeong HE, Lee JK, Kwak MK, Moon SH, Suh KY. Effect of leaning angle of gecko-inspired slanted polymer nanohairs on dry adhesion. *Appl. Phys. Lett.* 2010;96:043704.
- [25] Koros W, Stannett V, Hopfenberg H. Estimation of the effective permeability of thin surface layers created by exposure of polyethylene to fluorine. *Polym. Eng. Sci.* 1982;22:738–746.
- [26] Hougham G, Cassidy P, Johns K, Davidson T. 1999. *Fluoropolymers 1: synthesis and fluoropolymers 2: Properties*. New York, NY: Kluwer Academic/Plenum.
- [27] Kumar A, Hui CY. Numerical study of shearing of a microfibre during friction testing of a microfibre array. *Proc. R. Soc. A: Math., Phys. Eng. Sci.* 2011;467:1372.
- [28] Kim S, Sitti M, Hui C, Long R, Jagota A. Effect of backing layer thickness on adhesion of single-level elastomer fiber arrays. *Appl. Phys. Lett.* 2007;91:161905.
- [29] Murphy MP, Kim S, Sitti M. Enhanced adhesion by gecko-inspired hierarchical fibrillar adhesives. *Appl. Mater. Interfaces*. 2009;1:849–855.
- [30] Israelachvili JN. 2011. *Intermolecular and surface forces: revised third edition*. Academic press.
- [31] Autumn K, Dittmore A, Santos D, Spenko M, Cutkosky M. Frictional adhesion: a new angle on gecko attachment. *J. Exp. Biol.* 2006;209:3569–3579.
- [32] Del Campo A, Arzt E. Design parameters and current fabrication approaches for developing bioinspired dry adhesives. *Macromol. Biosci.* 2007;7:118–127.
- [33] Aksak B, Murphy MP, Sitti M. Adhesion of biologically inspired vertical and angled polymer microfiber arrays. *Langmuir*. 2007;23:3322–3332.
- [34] Long R, Hui CY, Kim S, Sitti M. Modeling the soft backing layer thickness effect on adhesion of elastic microfiber arrays. *J Appl. Phys.* 2008;104:044301–01-9.
- [35] Haiat G, Phan Huy M, Barthel E. The adhesive contact of viscoelastic spheres. *J. Mech. Phys. Solids*. 2003;51:69–99.
- [36] Aksak B, Murphy M, Sitti M. In: *Proceedings of the IEE International Conference on Robotics and Automation*; 2008; Pasadena, CA.
- [37] Abusomwan U, Sitti M. Effect of retraction speed on adhesion of elastomer fibrillar structures. *Appl. Phys. Lett.* 2012;101:211907.
- [38] Glassmaker N, Jagota A, Hui C, Noderer W, Chaudhury M. Biologically inspired crack trapping for enhanced adhesion. *Proc. Nat. Acad. Sci.* 2007;104:10786–10791.
- [39] Murphy M, Aksak B, Sitti M. Gecko inspired directional and controllable adhesion. *Small*. 2009;5:170–175.
- [40] Kim S, Aksak B, Sitti M. Enhanced friction of elastomer microfiber adhesives with spatulate tips. *Appl. Phys. Lett.* 2007;91:221913.